

University of Nevada, Reno

**Impact of Declustering on Probabilistic Seismic Hazard Estimates in the Western
United States**

A thesis submitted in partial fulfillment of the requirements for the degree of Master of Science in
Geophysics

by

Emily L. Maher

Dr. John Louie/Thesis Advisor

December, 2023



THE GRADUATE SCHOOL

We recommend that the thesis
prepared under our supervision by

entitled

be accepted in partial fulfillment of the
requirements for the degree of

Advisor

Committee Member

Graduate School Representative

Markus Kemmelmeier, Ph.D., Dean
Graduate School

Abstract

This study explores the relationship between declustering methods and earthquake hazard assessments, focusing on their implications for the USGS National Seismic Hazard Model (NSHM). Accurate seismic hazard analysis is crucial for informed decision-making and risk mitigation in engineering and urban planning.

The Zaliapin and Ben-Zion (ZBZ) declustering method, published in 2020, permits multiple iterations of declustering while maintaining the spatial distribution of background seismicity. It was employed to investigate the impact of retaining different proportions of background events in the catalog. Contour maps revealed that ZBZ and USGS declustering methods differ in their event removal patterns. The ZBZ method tended to remove events more densely clustered in areas with higher seismic activity, reflecting its sensitivity to local seismicity.

This study directly linked the number of retained background events in the catalog and earthquake hazard estimates. Maintaining approximately 38% of these events aligned hazard curves with USGS's results, indicating the practical significance of declustering in the creation of hazard assessments.

Variations from 10% to 90% of kept background events led an increase by nearly a factor of three in Peak Ground Acceleration (PGA) estimates. Underscoring the vital role of declustering in accurately characterizing earthquake hazards, especially when the proportion of background events varies.

In conclusion, this research advances the understanding of declustering's impact on earthquake hazard assessments, offering practical insights for enhancing accuracy. These findings contribute to seismology and can inform and improve earthquake preparedness and mitigation strategies. Future work includes expanding the analysis to larger datasets and exploring the effects of declustering in different geographic regions.

Table of Contents

<i>Introduction</i>	1
<i>Background</i>	3
<i>Objectives, Motivation, and Expected Outcomes</i>	8
<i>Coordination Work</i>	8
<i>Data</i>	9
c2 Catalog.....	10
c3 Catalog.....	10
<i>Methodology</i>	12
<i>Smoothing</i>	15
<i>Results</i>	17
Sensitivity to α_0	17
Contour Maps:.....	19
Hazard Curves:.....	23
<i>Discussion</i>	29
Contour Maps	29
Hazard Curves (Iterations).....	30
Hazard Curves Comparisons	31
<i>Conclusion</i>	31
<i>Summary</i>	32

<i>Suggested Follow Up Work</i>	33
<i>Data Used</i>	33
<i>References</i>	34
<i>Appendix</i>	36
Epicenter of Events with Time verse Latitude	36
Contour Maps showing where events are removed from catalog.	39
Hazard Curves with Multiple Catalog Realizations	42
Hazard Curve of ZBZ Method compared to Actual Curves and Estimate.....	45

List of Figures

Figure 1 - Table of parameters for the Gardner – Knopoff declustering method from GK (1976).

5

Figure 2 - Attraction domain of different magnitude earthquakes from Zaliapin and Ben-Zion (2020).

Showing the number of years that select earthquake magnitudes would affect a catalog's declustering.

6

Figure 3 - C2MAP & C2T-LAT: Epicenters of earthquakes for the c2 catalog along with a scatter plot of time versus latitude of the same catalog. 10

Figure 4 - Epicenters of earthquakes for the c3 catalog along with a scatter plot of time versus latitude of the same catalog. Notice the time-latitude plot of the declustered catalog has less intense dark horizontal streaks- the effect of removing aftershock 11

Figure 5 - C2MAG-T: Magnitude versus time for the initial c2 catalog. This figure shows completeness of the catalog increasing with time. 12

Figure 6 - α_0 -BACK: This figure shows the relationship between α_0 and the percentage of background events. 15

Figure 7 - Epicenters of the ZBZ catalog with 10% of background events kept. Adjacent to a scatter plot of the same catalog epicenters plotted against latitude versus years. 18

Figure 8 - Epicenters of the ZBZ catalog with 50% of background events kept. Adjacent to a scatter plot of the same catalog epicenters plotted against latitude versus years. 18

Figure 9 - Epicenters of the ZBZ catalog with 90% of background events kept. Adjacent to a scatter plot of the same catalog epicenters plotted against latitude versus years. 19

Figure 10 - Contour map of ZBZ declustered catalog removing 10% of background events from the c2 catalog. This depicts where the ZBZ declustering method removes earthquakes. 20

Figure 11 - Contour map of ZBZ declustered catalog removing 50% of background events from the c2 catalog. This depicts where the ZBZ declustering method removes earthquakes. 20

Figure 12 - Contour map of ZBZ declustered catalog removing 90% of background events from the c2 catalog. This depicts where the ZBZ declustering method removes earthquakes. 21

Figure 13 - Contour map of the USGS c3 declustered catalog from the c2 catalog. This depicts where the ZBZ declustering method removes earthquakes. 22

Figure 14 - Contour map of ZBZ declustered catalog removing 38% of background events from the c2 catalog. To compare the same amount of events removed by the USGS declustering versus the ZBZ declustering. This depicts where the ZBZ declustering method removes earthquakes. 23

Figure 15 - Epicenter of Monte Cristo Range Earthquake. 24

Figure 16 - Hazard Curve for Monte Cristo Range earthquake created with the USGS c3 catalog. 24

Figure 17 - Hazard Curve of 10% of events removed from seismic catalog. The green lines represent 100 different realizations of 10% of events being removed. Standard deviation is shown by the dotted lines, and the average is the solid black line. 25

Figure 18 - Hazard Curve of 50% of events removed from seismic catalog. The green lines represent 100 different realizations of 50% of events being removed. Standard deviation is shown by the dotted lines, and the average is the solid black line. 25

Figure 19 - Hazard Curve of 90% of events removed from seismic catalog. The green lines represent 100 different realizations of 90% of events being removed. Standard deviation is shown by the dotted lines, and the average is the solid black line. 26

Figure 20 - This is the coefficient of variation (σ/μ) versus α_0 of the estimated PGA at 2% exceedance probability in 50 years. Depicting that as α_0 increases there is less variation in the data. 26

Figure 21- This graph shows the average exceedance rates for all of the 100 runs per percentage of catalog kept along with the standard deviation values. As the number of events in the catalog increases, the variability in the data decreases. 27

Figure 22 - This depicts hazard curves of 10% of the seismic catalog removed. The John Anderson smoothing algorithm simplifies the complicated logic tree the USGS uses to predict hazard. This plot comparison relays the simplification is reasonable. 28

Figure 23 - This depicts hazard curves of 50% of the seismic catalog removed. The John Anderson smoothing algorithm simplifies the complicated logic tree the USGS uses to predict hazard. This plot comparison relays the simplification is reasonable. 28

Figure 24 - This depicts hazard curves of 90% of the seismic catalog removed. The John Anderson smoothing algorithm simplifies the complicated logic tree the USGS uses to predict hazard. This plot comparison relays the simplification is reasonable. 29

Introduction

In areas with high earthquake probabilities, the risk of damage to anthropogenic structures is elevated. The damage to these buildings could be a result of large ground motion caused by P and S-waves. Probabilistic seismic hazard maps are available to guide professionals when developing building codes for structures to be built in designated “high risk” zones. These probabilistic seismic hazard maps have been created since 1976 to assist private and public entities develop policies for earthquake-safety. These maps continue to be used in the design process of structures and facilities (Peterson, 2020). The probability of earthquake ground motion surpassing a given value in a given location is the basic premise of this classification method (Cornell, 1968; Reiter, 1990).

An example of these probabilistic seismic hazard maps is the U.S. National Seismic Hazard Map (NSHM) (Peterson, et. al., 2020). It is time-independent and used across the United States to assist professionals in planning and building structures. Time independence is based on the assumption that seismic activity stays consistent over an extended period. Many different components factor into the creation of a NSHM. The NSHM considers multiple hazard curves (Peterson, 2020). A *hazard curve* is a graph depicting ground accelerations and their probability of exceedance (e.g., 2%) of a specific value during a specified time frame (e.g., 50 years). These hazard curves are created using different seismic source characterizations and ground motion estimates (Budnitz, 1997).

To create a seismic hazard curve, scientists first gather historical earthquake data, geological insights, and seismological information to estimate the likelihood of earthquakes of differing magnitudes occurring in a given area. These probabilities are then plotted against the corresponding ground shaking intensities on a *hazard curve*, with the y-axis representing the annual probability of exceeding a particular intensity level. Hazard at a pre-selected exceedance

rate is calculated at points that are determined by a virtual grid set over a particular area. The ground motions for each exceedance rate are then linked together to show the change in hazard.

In areas like Nevada, where historical earthquake records may not fully capture ground motions for large earthquakes, extrapolation techniques are employed to estimate ground accelerations for earthquake magnitudes higher than those observed in historical records. Probabilistic Seismic Hazard Analysis (PSHA) uses Ground Motion Prediction Equations (GMPEs) empirical relationships to correlate earthquake magnitude, distance from the source, and local geological site conditions to predict ground motions. GMPEs, used in areas with insufficient data, are created using data from large seismic events in different areas with high rates of seismic activity (Budnitz, 1997). While these extrapolation methods provide valuable insights, they come with uncertainties, and it remains essential to monitor seismic activity and collect data to refine and validate the estimates for improved seismic hazard assessments in the region.

Efforts have been made to improve the accuracy of probabilistic seismic hazard analysis by declustering the catalog of acceleration data recorded during historic seismic events (Zaliapin and Ben-Zion, 2020). Declustering is the process of removing dependent seismic events, resulting in a catalog composed of independent events only (Van Stiphout et. al., 2012). *Independent events*, defined as significant initial events (seismic mainshocks), can "stand alone," meaning there was not a previously observed event that could have caused it. In contrast, *dependent events* are earthquakes that independent events trigger. These are also known as fore- or aftershocks. It is crucial to note that declustering is not a standardized process. The choice of declustering method and associated assumptions can significantly affect the composition of the resulting seismic catalog. I hypothesize varying composition of the catalog will lead to varying seismic hazard curves. Different probabilistic seismic hazard curves could impact the design of structures built under consideration of the updated data (United States Geologic Survey, 2019).

The study presented in this thesis focuses on the evaluation of the effects of the Zaliapin & Ben-Zion (2020; “ZBZ”) method of declustering on available seismic hazard curves for zones in the Western U.S. Though there are many different declustering methods (Van Stiphout et. al., 2012), the ZBZ method was chosen due to its user friendliness: ZBZ users can easily change controlling parameters and assumptions quickly, which allows studying the effect of each parameter and assumption modification on the composition of the declustered seismic catalog. In this study, the focus is put on the effect of modifying a specific parameter of the ZBZ declustering method. The parameter of interest is a variable that determines how many events are kept in the declustered catalog. In further course of this thesis, this parameter is referred to as α_0 .

Note that this study is focused on the effect of α_0 on the composition of the seismic catalog declustered using the ZBZ method. For an in-depth review of the ZBZ method, the I refer to the available literature (Zaliapin & Ben-Zion, 2020).

Background

Earthquake hazard refers to the potential threat posed by seismic activity in a given region, encompassing the likelihood and intensity of ground shaking resulting from tectonic movements beneath the Earth's surface. Understanding earthquake hazards is crucial for assessing and mitigating risks to human life, infrastructure, and the environment. Primary hazards that are caused by earthquakes include ground shaking, landslides, liquefaction, and surface rupture, with secondary effects ranging from tsunamis to flooding and fires (Pacific Northwest Seismic Network, 2023). All these effects require different infrastructure to mitigate the effect of these possible outcomes from an earthquake. Seismic hazard maps play an important role in this process by visually representing the varying levels of earthquake risk across a geographic area. These maps integrate complex data, including historical earthquake records, geological information, and sophisticated seismic models, to depict the probability of ground shaking at different intensities over time. These maps assist urban planners, engineers, and policymakers in

making informed decisions regarding land-use planning, building design, and emergency preparedness. They serve as essential tools for developing and implementing effective strategies to enhance the resilience of communities in earthquake-prone regions, ultimately contributing to the safety and sustainability of urban environments (Peterson, 2020).

The United States Geological Survey, USGS, is a department in the United States Department of Interior that supports science for earthquake hazard as well as other natural hazards within the U.S. An updated National Seismic Hazard Model is published every four years. This report includes a new Hazard Map. Earth scientists across the United States contribute to the model's updates (Peterson et. al., 2019).

When making seismic hazard maps this group utilizes the Gardner and Knopoff method (from here on referred to as G.K.) in their 2014 declustering effort to update NSHM. This declustering method is one of the original techniques. Developed in 1974, this method built a foundation for declustering procedures developed since (Van Stiphout et. al., 2012). The general methodology of declustering is explained in the following.

Independent events, also known as “mainshocks”, can be characterized as the events with the most significant magnitudes (according to Richter scale) at a specified location during a specified duration (i.e., in a “time-space window”). Aftershocks, commonly called “secondary events”, are defined as events with smaller lower magnitudes than main shocks. Aftershocks are triggered by mainshocks, and are therefore, per definition, not independent. An earthquake sequence is a group or cluster of earthquakes that includes a single mainshock followed by one or more aftershocks. Declustering methods are used to distinguish between mainshocks and aftershocks.

Declustering of seismic hazard catalogs should not be viewed as a unique solution to remove dependent events from a seismic catalog. The resulting catalog composition is influenced by the choice of declustering method (Christopherson et. al., 2011) as well as the choice of parameters and assumptions made. Earthquake sequences are naturally occurring events, and there is no distinctive feature indicating where the boundary between a mainshock and when aftershocks

begin (ZBZ, 2020). This boundary determination generally varies with what type of declustering application is used creating a bias for different algorithms.

This bias can be demonstrated on the basis of the GK method, which is a deterministic window method. Deterministic window methods generate results based on the parameters a user sets rather than the data set itself. A user selects a time and space limit, this then determines if an event is independent or dependent. These limits are utilized to compute a time-space window. One independent variable in these methods is the recorded peak earthquake magnitude during the analyzed earthquake sequence. Once a time-space window is computed, this window is used to determine which events are dependent and which are independent within the seismic sequence. Eventually, this distinction is made to determine which events are removed from the seismic catalog.

Each earthquake magnitude has its own “space” and “time” criterion to determine the surrounding window in which events will be removed. The data used by GK to determine the time-space window based on the earthquake magnitude are shown in Table 1. The values in this table are merely recommendations, as the authors propose that users employ whatever parameters they feel necessary. Parameters may be changed based upon the geographic location, existence of faults, and previously recorded seismic activity.

TABLE 1
WINDOW ALGORITHM FOR AFTERSHOCKS

<i>M</i>	<i>L</i> (km)	<i>T</i> (days)
2.5	19.5	6.
3.0	22.5	11.5
3.5	26.	22.
4.0	30.	42.
4.5	35.	83.
5.0	40.	155.
5.5	47.	290.
6.0	54.	510.
6.5	61.	790.
7.0	70.	915.
7.5	81.	960.
8.0	94.	985.

Figure 1 - Table of parameters for the Gardner – Knopff declustering method from GK (1976).

By using set time/space windows, events that fall within the aftershock zone and are under a certain magnitude are removed. Consequentially, there can be a period of time after a mainshock during which all events are excluded. Colloquially, this data gap is called a "hole." This hole is caused by removing all events within the aftershock zone.

The attraction domain, the data gap mentioned above, is the spatial and temporal period after a sizeable earthquake. The larger the event, the wider the range of events eliminated from the catalog. With a windowing method, the attraction domain of more significant earthquakes affects the declustered catalogs. Figure 2 below from Zaliapin and Ben-Zion (2020) depicts how this data gap can affect the catalog. Magnitudes are represented on the x-axis and latitudes on the y-axis. The larger the magnitude, the more significant the effect on the data set, represented by the colored shapes in the graph. The colored area after the event covers the latitude and magnitude of events removed from the catalog.

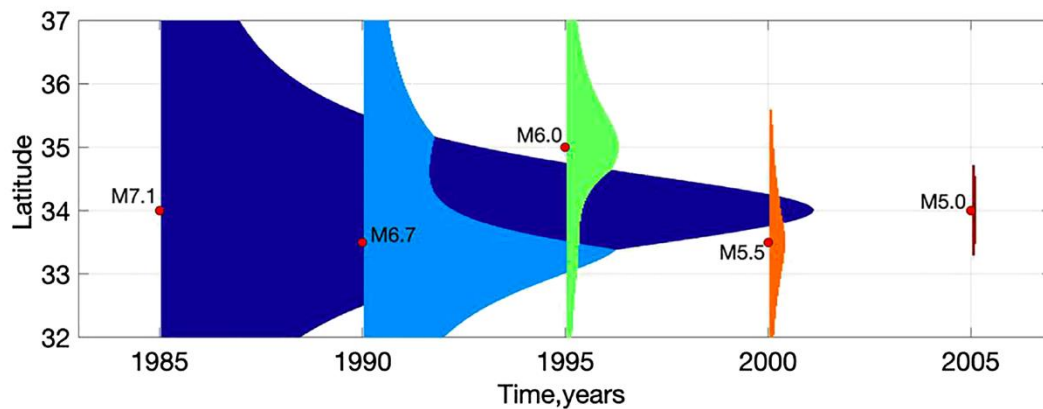


Figure 2 - Attraction domain of different magnitude earthquakes from Zaliapin and Ben-Zion (2020). Showing the number of years that select earthquake magnitudes would affect a catalog's declustering.

With the GK method, the time space windows create holes after large events. It can be assumed that independent events are removed from the catalog (van Stiphout, 2012). However, GK hypothesize that a fairly limited number of events were removed from the tested seismic catalog. This would lead to an overestimation in predicted hazard. When earthquake hazard is

simplified, hazard is equal to the seismicity rate times the number of events represented by the following equation:

$$H = R * N \quad (1)$$

Where H is the hazard, R is seismicity rate (number of earthquakes exceeding a specified magnitude), and N as the number of earthquakes in a catalog above the specified magnitude. Equation 1 shows that if the number of events kept in a catalog increases so will the predicted hazard.

Other declustering methods, such as the one developed by Reasenberg et al. (1985) go a step further than GK by linking the triggering of aftershocks to independent events. These grouped earthquakes can be referred to as clusters. This cluster-linking method is similar to GK as a user sets the parameters for the data set rather than the data set defining them.

Another cluster-linking method, by Zhuang et al. focuses on dependent events being space dependent, but not time. This method is more sophisticated than the GK method, being a space-time branching stochastic model. The analysis uses the Epidemic Type Aftershock Sequence (ETAS) model to define the best space-time window parameters for a given data set and sets a probability of each earthquake being dependent upon all preceding events. The ETAS modal sets a limit of parameterized space-time distance for an event being paired to a previous event with a time-space window (van Stiphout, 2012).

Zaliapin and Ben-Zion (2008) created their method which identifies background earthquakes on a space-time graphical representation of distance. This is built off of a method by Marco Baiesi and Maya Paczuski (BP) which defines the clustering of earthquakes. This is published in their 2004 paper, *Scale-free networks of earthquakes and aftershocks*. Clustering earthquakes better defines the nature of seismic activity and linking events together based upon a relationship of being a main or aftershock. In their works from 2008 and 2013, ZBZ employed a framework

that utilizes a nearest-neighbor analysis to define earthquake clusters, incorporating both spatial and temporal dimensions. This method calculates pairwise distances between seismic events, identifying the events that are most closely related. Within this framework, ZBZ introduced the concept of pairwise earthquake distance, denoted as η_{ij} .

The work previously done by these researchers on defining earthquake clustering behavior led to the declustering method used for this study. Zaliapin and Ben-Zion (2020) proposed a nearest-neighbor randomly thinning stochastic method. This stochastic method surveys seismic events on a time and distance scale and uses random reshuffling to thin the seismic catalog (Zaliapin and Ben-Zion, 2020). The random thinning of the catalog allows the new record to be less affected by outliers in the data.

The reason I chose to use the ZBZ to test declustering is based on the following reasons: it is easy to adjust the number of events that are deemed independent in a catalog and each time a test is run the catalog is randomly thinned. Randomly thinning the catalog is important when determining the effect of declustering as it removes events that could be outliers. An outlier being an event that could be at an unusual depth, have a larger than normal magnitude, or have an odd location.

Objectives, Motivation, and Expected Outcomes

Within this thesis I test how different numbers of events kept in a seismic catalog affect the hazard. More so how the different number of events defined as background affect the hazard curves. To test this, I ran the ZBZ declustering method 100 times at the same α_0 value. This returns a different catalog every time because of the random thinning. With different percentages kept and then averaged into a single curve I determine how the number of events effect hazard. I compare my declustered catalog to the USGS declustered catalog to see how my results align with the GK declustering method. The area of study is the Western United States.

Coordination Work

My study builds upon the work of John Anderson and Ilia Zaliapin, who initiated the grant proposal and completed the technical report "*Final Technical Report USGS Award Number G20AP00010 Effects of Earthquake Declustering on the US National Seismic Hazard Maps. (2023)*" As a contributor to the project, I played a key role in the initial stages of data analysis by collecting and preparing the catalogs used in the study.

For calculating the displayed hazard curves, I employed a personalized algorithm developed by John Anderson, which provides a simplified representation of the hazard curves used in the National Seismic Hazard Model (NSHM). To ensure a refined catalog, I applied a declustering algorithm to the data, resulting in a thinned catalog that was subsequently smoothed. Employing Anderson's simplified hazard curve program, I focused on analyzing the impact of different catalog thinning methods on the hazard of specific locations characterized by low background seismicity, rather than multiple locations. Additionally, the study compared the event removal methods of the ZBZ method from a seismic catalog and the GK declustered catalog utilized by the USGS.

One of the main contributions of this research was the idea to employ percentages of the catalog to assess the influence of seismic catalogs on hazard curves. For this investigation, 100 realizations of the catalog were created.

It is important to note that some discrepancies exist between the catalogs utilized in my study and those employed in previous work. Specifically, this thesis applied a moment magnitude cutoff of 3.5, while the technical report used a cutoff of 4.0. Moreover, the Maximum Shaking Earthquake Catalog (MSEQ) was not used in any of the results. By addressing these variations, this research enhances our understanding of seismic hazard assessment and its implications for specific locations with low background seismic activity.

Data

This study uses two publicly available seismic catalogs to demonstrate the effect of declustering. Readers should also note that we focused on the Western United States for this study. The Central and Eastern United States have a separate catalog. These catalogs are available through sciencebase.gov, and links provided at the end.

c2 Catalog

c2 is a raw catalog. This catalog is "cleaned" but not declustered. In the process of cleaning a catalog, all duplicate events and events deemed anthropogenic are deleted. Hazard analysis excludes events with a moment magnitude (M_w) less than 3.5. Moment magnitude is an earthquake classification method that classifies event size based on multiple physical attributes of the event. This is the same raw catalog used for the 2018 National Seismic Hazard Model, ranging from 1850 to 2016. This study utilizes the c2 catalog for its analysis. The total number of events in the catalog was 13,812. The locations of the c2 events are depicted in the map of Figure 3 - C2MAP. Figure 3 - C2T-LAT depicts the time versus latitude over the time duration of 166 years.

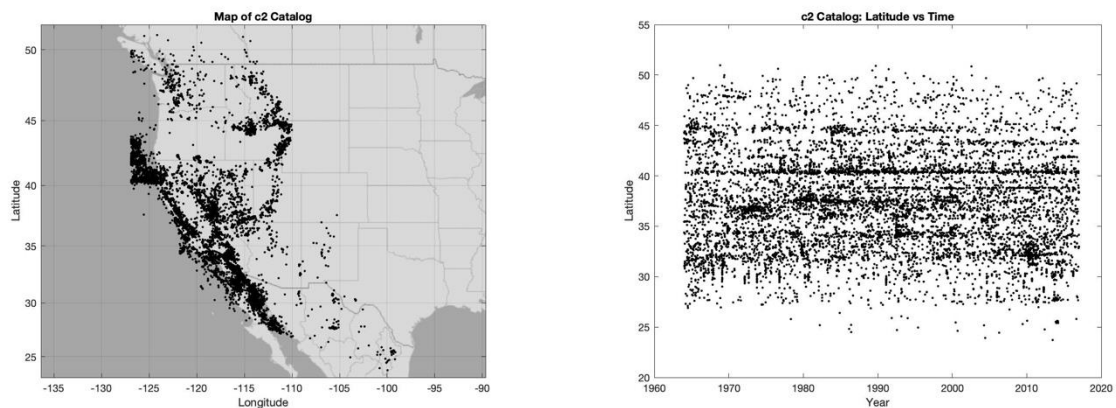


Figure 3 - C2MAP & C2T-LAT: Epicenters of earthquakes for the c2 catalog along with a scatter plot of time versus latitude of the same catalog.

c3 Catalog

I use the USGS's declustered catalog to compare this study's declustering method to what was produced for an NSHM. The USGS declustered catalog is referred to as c3. It also has a year range from 1850 to 2016 and events with a moment magnitude larger than 3.5. Figure 4: C3T-LAT depicts the time versus latitude over the time duration of 166 years.

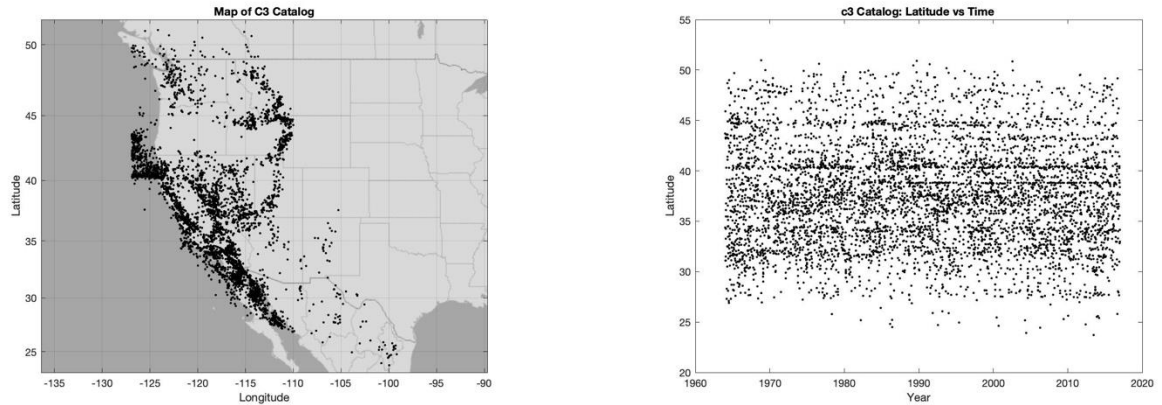


Figure 4 - Epicenters of earthquakes for the c3 catalog along with a scatter plot of time versus latitude of the same catalog. Notice the time-latitude plot of the declustered catalog has less intense dark horizontal streaks- the effect of removing aftershock.

When declustering with the ZBZ Method, I start with the c2 raw catalog. Figure 5: C2MAG-T depicts the entire c2 catalog from 1769 to 2016 with magnitude vs. time. In this figure, the density in the catalog of events with a magnitude below ~ 3.5 and the density of events occurring after the mid-1960s increase significantly. The increase in density can be attributed to the advancement of seismic monitoring capabilities. I cut the data from 1964 to 2016 and only analyzed events above magnitude 3.5. The 1964-year cutoff is determined by observing the "completeness" in a scatter plot with the earthquakes plotted over time versus latitude. A significant jump in the number of events above magnitude 3.5 after 1964 gives weight to using this period. This magnitude cutoff was chosen with the hopes of working with the most complete catalog as earthquake monitoring has improved, creating a more thorough one.

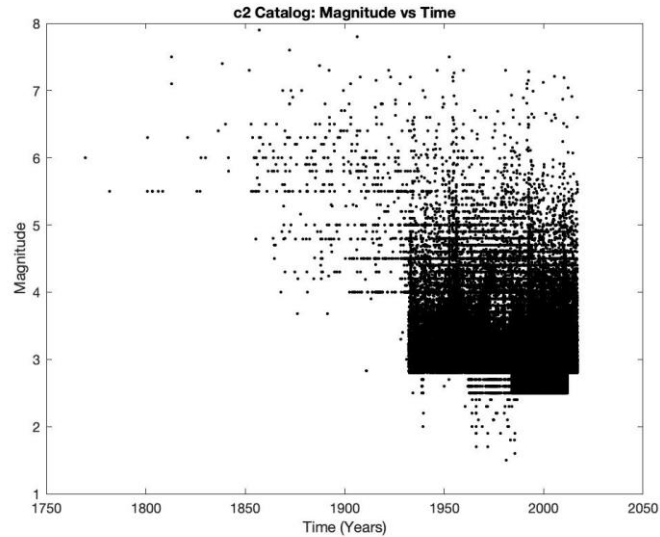


Figure 5 - C2MAG-T: Magnitude versus time for the initial c2 catalog. This figure shows completeness of the catalog increasing with time.

Methodology

The primary declustering method utilized during this study is the Zaliapin Ben-Zion (ZBZ) nearest neighbor declustering method published in 2020. This stochastic declustering method randomly thins the seismic catalog while preserving the spatially inhomogeneous rate of background events. Background events are earthquakes that occur naturally within a region or time period where seismic activity is typical. Background seismic events are not associated with a significant "trigger" event, meaning they are independent. Due to randomization, a different set of events classifies as independent for each realization; the ZBZ algorithm allows for creating multiple declustered versions of a single seismic catalog.

The ZBZ method begins with finding the most prominent clusters in a seismic catalog. The algorithm determines each earthquake's nearest neighbor (i.e., the nearest alternative seismic event) based on the spatial distribution of all events included in the catalog. This seismic cluster analysis is explained in more detail in Zaliapin & Ben-Zion (2013a): Each event is assigned a

nearest neighbor proximity value, η . This value depends upon the event's location, time, and magnitude. Equation (1) is used to determine the value of η .

$$\eta_{ij} = \begin{cases} t_{ij}(r_{ij})^d 10^{-wm_i}, & t_{ij} > 0; \\ \infty, & t_{ij} \leq 0 \end{cases} \quad (1)$$

Where j represents the offspring event of the defined parent event, i . t is the occurrence time of the event, m – magnitude, d – fractal dimension of the hypocenter, r – spatial distance between hypocenters.

The Gutenberg-Richter law (GR) is used to determine w . w is the b-value from GR, defined with the equation below.

$$\log_{10}N(m) = a - bm, b \approx 1, m \geq m_c \quad (2)$$

(a a constant) w is the parameter which weights events, i , based on its magnitude.

$$\eta_j = \min(\eta_{ij}, i < j) \quad (3)$$

Each event, j event is linked to a parent, i , using the equation above. This is done by using the events defined with the nearest neighbor proximity, equation (1). d is set to 1.5, and w is set to 0.5. Each event in the catalog, excluding the first, is related to previous event. The data of the time and space relationships between i events and j events are normalized through magnitude by the following equations:

$$T_{ij} = t_{ij}10^{-qwm}; \quad R_{ij} = (r_{ij})^d 10^{-pwm}; \quad q + p = 1 \quad (4)$$

This step removes events that are heavily clustered. Meaning removing parent events, i , with a nearest neighbor proximity less than the set value. This is done because aftershocks tend to occur as a group and along a fault geometry after a large-scale seismic event.

$$\{i(j) : \eta_{i(j)} > \eta_0\}, j = 1, \dots, N_0 \quad (5)$$

Each event in the catalog is assigned a *proximity measure* alpha (α). α is a normalized nearest-neighbor proximity value computed by scaling the nearest-neighbor proximity (η_j) to the

estimated background intensity. An estimated probability that controls the number of events kept in the catalog is independent and parameterized with the threshold, α_0 .

α_0 controls the random thinning of the catalog. By randomly thinning the catalog, events that have short proximities to large events may remain. Random thinning of a seismic catalog is important when declustering because it can help to reduce the influence of large seismic events in the analysis. This also creates a more realistic event distribution after a large mainshock, where holes were left when using a method like Gardner and Knopoff (1974).

With multiple realizations of the catalog, we vary the background seismicity kept in the catalog. Multiple random realizations of declustering can be produced for a given α_0 . Varying the threshold, α_0 , to create multiple iterations of catalogs allows for keeping different percentages of background events, ranging from 10% to 90%. By changing α_0 , an event classifies as either independent or dependent by where its α value falls in relation to α_0 .

It is important to note that with each catalog iteration, the events composing the catalog vary. This study does not show the entire span of declustering outcomes but rather how different declusterings affect hazard.

As the value of α_0 changes, the number of events kept in the catalog shifts as well. The smaller the value α_0 , the more background events are kept in the catalog. The percentage of background events represents the number of seismic events kept from the original catalog. Figure 6: α_0 -BACK shows the correlation of background events kept versus α_0 values.

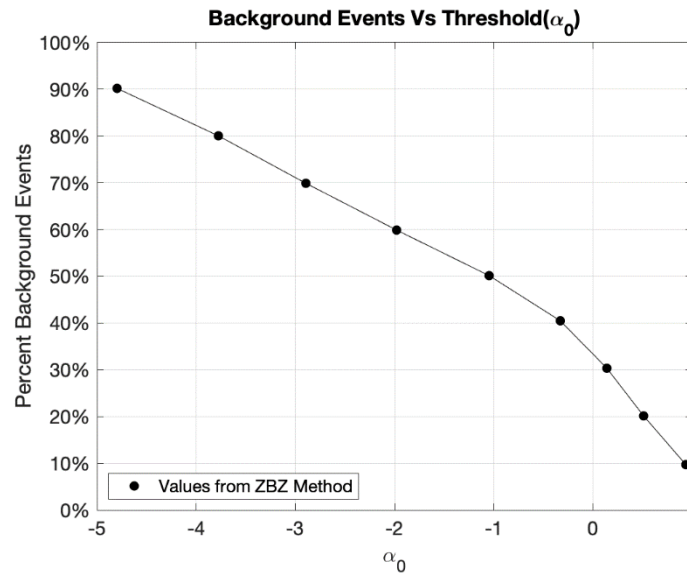


Figure 6 - α_0 -BACK: This figure shows the relationship between α_0 and the percentage of background events.

Smoothing

Following the steps to create a hazard model, I apply a smoothing algorithm to the catalog. An agrid is an imaginary box that is laid across the study area; these represent the seismic frequency of earthquake occurrences in the area. By creating these boxes over the area, uncertainties in the seismic catalog are accounted for. These grids are created and used to have a type of forecast for the select 0.1° latitude by 0.1° longitude square.

The USGS utilizes a complicated logic tree to make its agrids. Creating the same agrid is a complicated multistep process that would not fit in with the time allotted for this study. The agrids that need to be resembled are the California Agrids. California has many factors that play into the agrids, including UCERF3. This will need to be done in the next iteration, as the USGS will create agrids from now on. This process involves spatial probability density functions (PDF)—these scale around a selected a -value, creating the agrid (Peterson, et. al., 2020). To streamline this process, we use a simplified smoothing approach, which John Anderson created to make it easy to smooth a seismic catalog.

I set a 0.1° latitude by 0.1° longitude grid across the Western United States with a defined center point of each grid square. The algorithm defines the nearest neighbors for each event by determining the distance from the event to the center of the grid. If the distance of the earthquake to the center of the grid is three times greater than the measure of the distance from the earthquake to its fourth nearest neighbor, the event is added to the sum of events for that particular grid square. Normalizing the different distances of each event to one after all events are accounted for. Normalizing these distances is vital to reduce the effect of outliers on the data set while allowing for comparison between cells. This smoothing method was created by John Anderson for this and similar studies to simplify the process of smoothing, allowing multiple realizations to be created quickly.

Smoothing Equation:

The maps in Figures 7-10 DECL1-DECL3 depict where events have been removed in the declustering. Below are examples of the 10%, 50%, and 90% of events, the other percentages are attached in the appendix.

Color-contoured maps, Figures 11-13, represent the difference in the c2 and c3 catalogs. The maps depict the c3 catalog divided by the c2 catalog to depict where there are more events removed. The percentage is the percentage of the seismic catalog that is kept for further hazard analysis. These maps help determine where events are removed or kept.

After creating a grids, we use these data to generate hazard curves of given areas. Peak Ground Acceleration (PGA) is the maximum acceleration of the ground during an earthquake at a select location. This value is the x-axis of a hazard curve with the exceedance on the y-axis. The exceedance rate is the expected number of times per year a given ground motion is surpassed. These graphs contribute to the hazard map of an area.

The exceedance rate for the selected probability (say $P = 0.02$ or 2% in 50 years) relates to the hazard curve, $HC(PGA)$, by equation 6:

$$P(PGA) = 1 - e^{(-HC(PGA)*T)} \quad (6)$$

T is the duration time. For example, this variable would be set to T=50 years for an exceedance rate of 4.041×10^{-4} per year at a $P(PGA) = .02$.

The plots have a curve created from the 2018 Probabilistic Seismic Hazard Analysis, PSHA data set (Rukstales, K.S., and Petersen, M.D., 2019) to compare the ZBZ declustered hazard curve to the actual. An approximation curve is also created from our simplified smoothing, as the USGS has a complicated logic tree that factors in faults to make agrids. This estimated curve is the plot of the USGS data with the same smoothing process we used and the hazard curve from the ZBZ declustered catalogs. In Figures 22 through 25 these three lines plotted together show how the different catalogs stack up against each other.

Results

Sensitivity to α_0

The following figures depict the ZBZ declustered catalogs. The maps are the locations of seismic events deemed "independent" by the algorithm, while the Latitude vs. Time plots represent events kept over the time period. Each figure constitutes a different percentage of the catalog kept (10-90%).

The 2018 USGS c3 catalog has 5291 events within the time window we set, which correlates to 38% of background events kept in the c2 catalog. α_0 can easily be adjusted to generate specific percentages of background events kept in a catalog. To compare directly to USGS results, the α_0 the percentage of background events kept selected is 38%. This allows for a direct comparison to the 2018 USGS c3 catalog throughout the results.

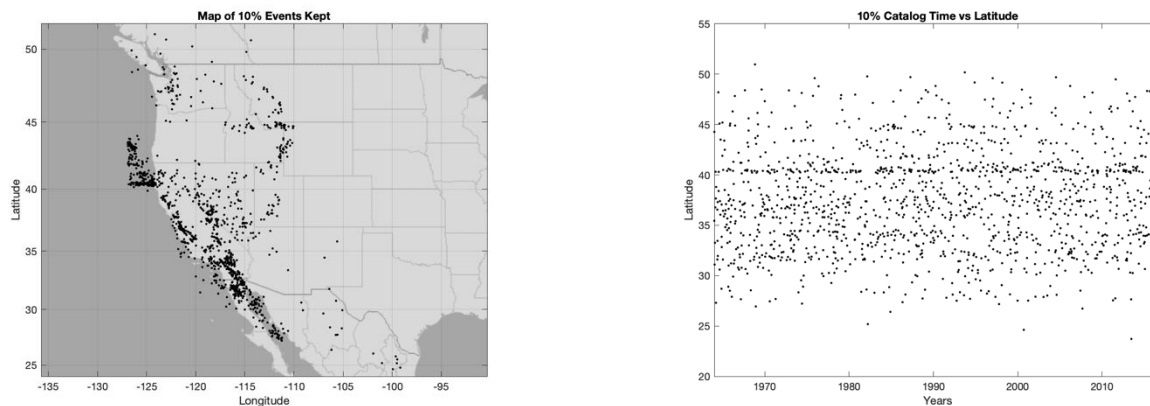


Figure 7 - Epicenters of the ZBZ catalog with 10% of background events kept. Adjacent to a scatter plot of the same catalog epicenters plotted against latitude versus years.

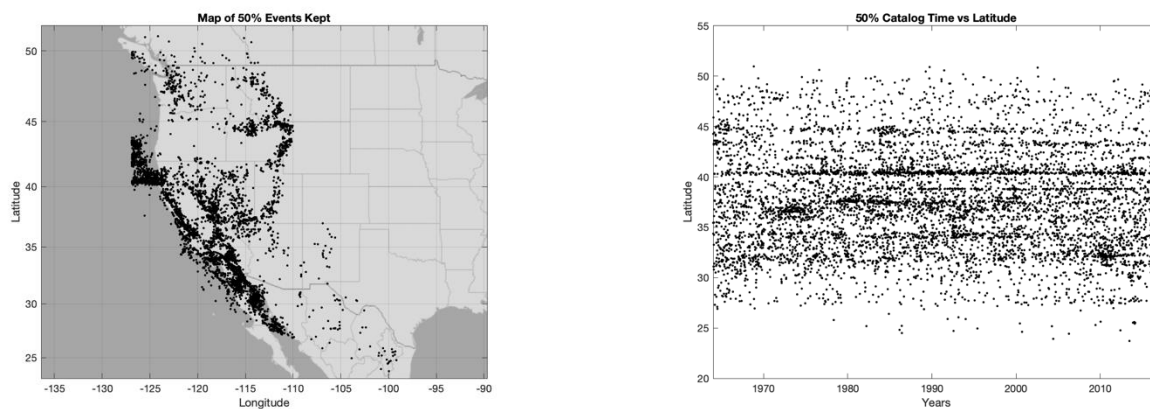


Figure 8 - Epicenters of the ZBZ catalog with 50% of background events kept. Adjacent to a scatter plot of the same catalog epicenters plotted against latitude versus years.

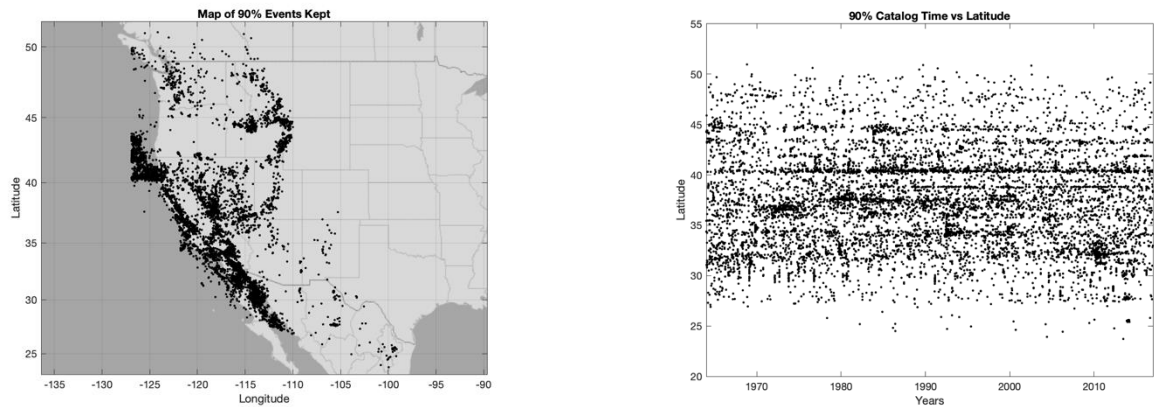


Figure 9 - Epicenters of the ZBZ catalog with 90% of background events kept. Adjacent to a scatter plot of the same catalog epicenters plotted against latitude versus years.

Contour Maps:

In these figures, red represents the most significant percentage of events removed from the c2 catalog. Where there is dark blue or white, there is either no data present or no events have been removed.

The 10% of events removed in the catalog map either has dark blue, no data or events removed, or light blue showing small amounts of the catalog have been removed. With the smaller catalog size, the deemed independent events would be in seismic "hot spots." The algorithm keeps the unquestioned independent events. So, there is either no data - dark blue - or a small percentage of the catalog removed.

As the number of events kept in the catalog rises, there is an increase in the number of events removed. The range of events in the catalog will vary more, as the α 0 value is higher and, therefore, less picky about labeling events "independent".

With the smaller catalog size, the events deemed independent would be in seismic "hot spots."

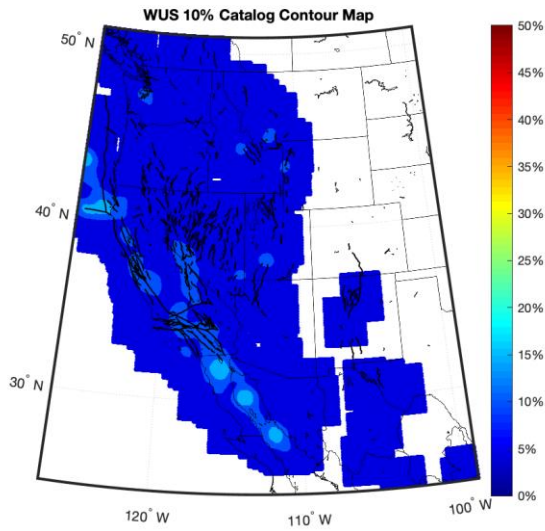


Figure 10 - Contour map of ZBZ declustered catalog removing 10% of background events from the c2 catalog. This depicts where the ZBZ declustering method removes earthquakes.

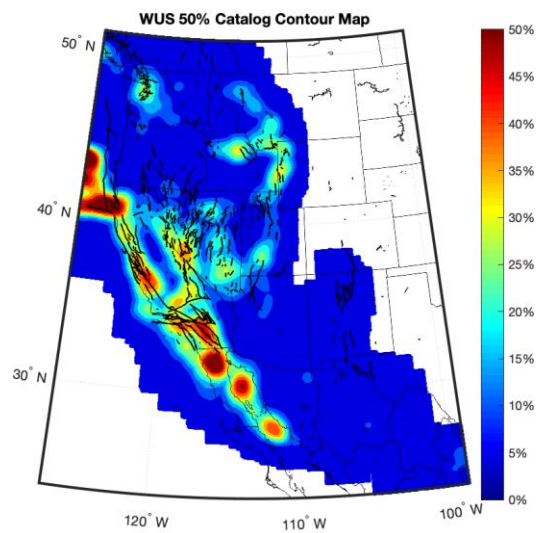


Figure 11 - Contour map of ZBZ declustered catalog removing 50% of background events from the c2 catalog. This depicts where the ZBZ declustering method removes earthquakes.

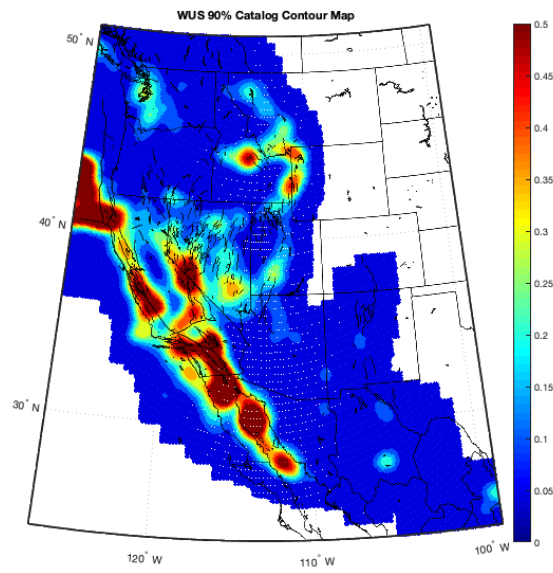


Figure 12 - Contour map of ZBZ declustered catalog removing 90% of background events from the c2 catalog. This depicts where the ZBZ declustering method removes earthquakes.

Comparing the USGS c3 catalog contour to the 38% ZBZ catalog contour depicts the difference in declustering methods. There are noticeable differences between the two maps. The differences are caused by the way in which the data is declustered, windowing vs. nearest-neighbor. The USGS catalog has fewer events removed in seismically heavy areas. There are more/larger areas with 20-30% of events removed rather than the 38% catalog. The 38% catalog has more concentrated areas of events removed – displayed by the dark red. These concentrated

areas trend through all of the ZBZ declusterings. The ZBZ algorithm removes more events where there are higher concentrated areas of events.

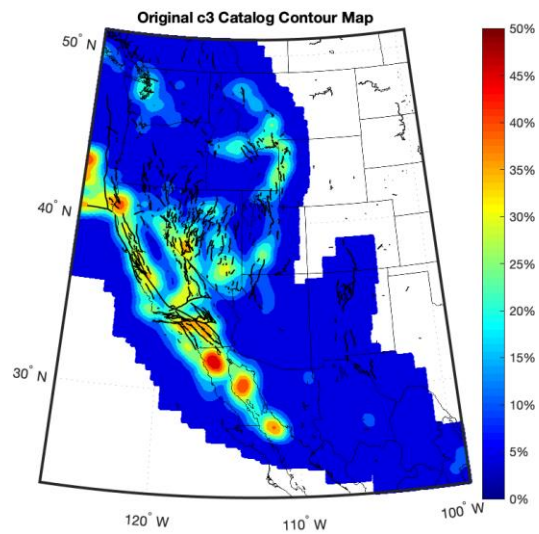


Figure 13 - Contour map of the USGS c3 declustered catalog from the c2 catalog. This depicts where the ZBZ declustering method removes earthquakes.

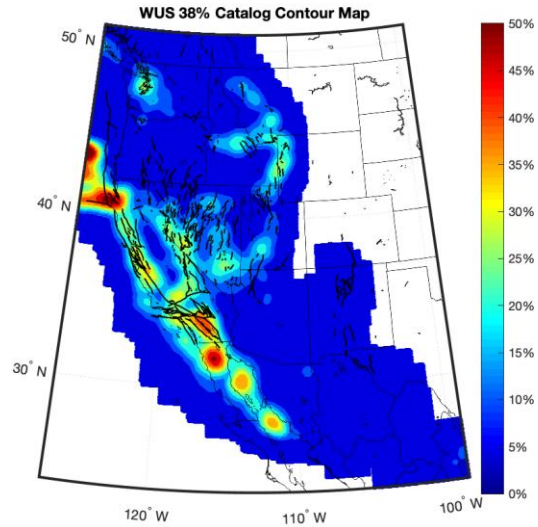


Figure 14 - Contour map of ZBZ declustered catalog removing 38% of background events from the c2 catalog. To compare the same amount of events removed by the USGS declustering versus the ZBZ declustering. This depicts where the ZBZ declustering method removes earthquakes.

Hazard Curves:

For determining how declustering affects hazard curves, it was essential to select an area with no significant fault that could be contributing to the seismicity of the area. This would allow for the events recorded to be classified as background seismicity. On May 15, 2020, at 4:03:27 AM PST, a Mw 6.5 earthquake occurred in the Monte Cristo Range in central Nevada. The location of this earthquake was chosen as the location to compare the seismic hazard curves. Below, Figure 14, is a map of the event's origin and the hazard curve from the USGS for this location.

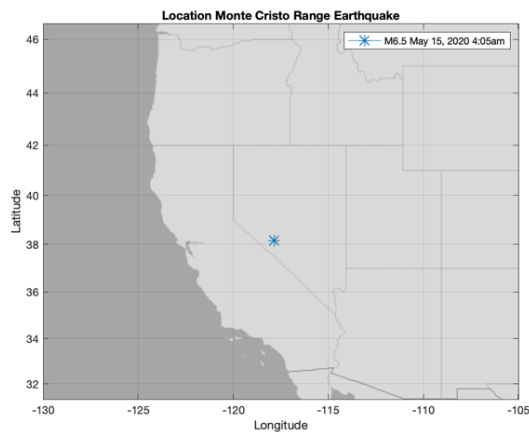


Figure 15 - Epicenter of Monte Cristo Range Earthquake.

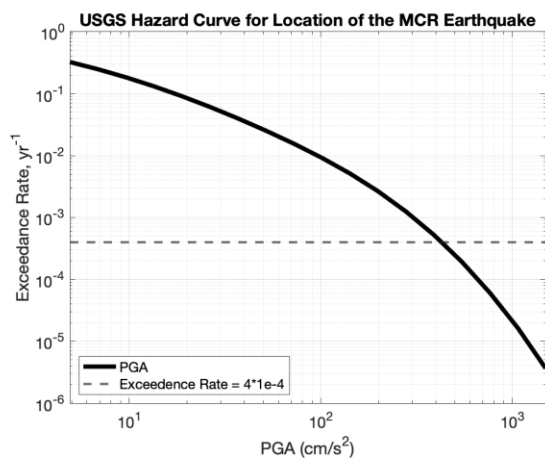


Figure 16 - Hazard Curve for Monte Cristo Range earthquake created with the USGS c3 catalog.

The following graphs depict hazard curves from 100 different iterations of the same catalog percentage. One hundred iterations are utilized to demonstrate the effects of random thinning on a catalog. As the number of events kept in the catalog increases, the variability in the hazard curves decreases. In the following graphs, the different iterations of the catalog are colored green, the standard deviations (σ) are the dotted lines, and the mean (μ) is the solid black line. The horizontal grey line is an exceedance rate of 4×10^{-4} ; this would be an estimated PGA at 2% exceedance probability in 50 years.

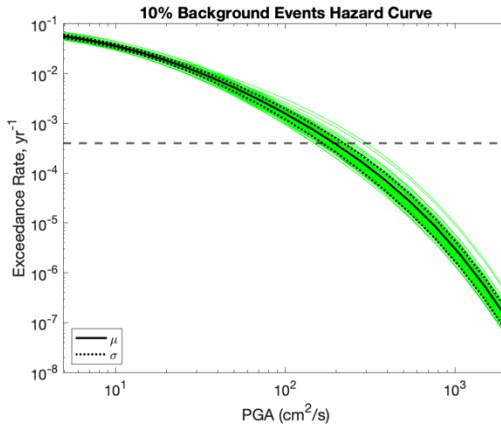


Figure 17 - Hazard Curve of 10% of events removed from seismic catalog. The green lines represent 100 different realizations of 10% of events being removed. Standard deviation is shown by the dotted lines, and the average is the solid black line.

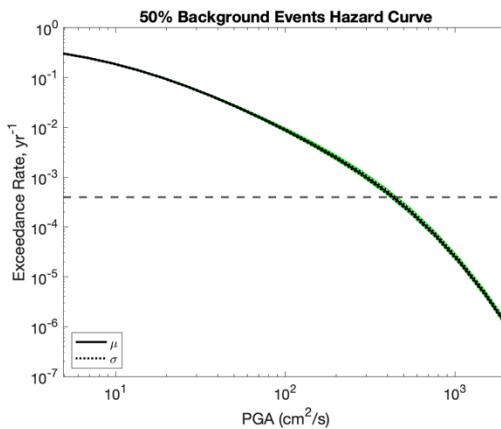


Figure 18 - Hazard Curve of 50% of events removed from seismic catalog. The green lines represent 100 different realizations of 50% of events being removed. Standard deviation is shown by the dotted lines, and the average is the solid black line.

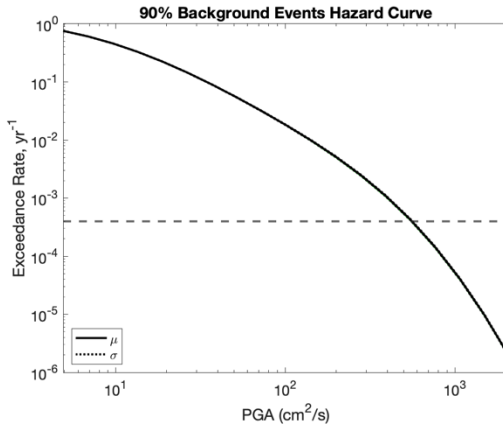


Figure 19 - Hazard Curve of 90% of events removed from seismic catalog. The green lines represent 100 different realizations of 90% of events being removed. Standard deviation is shown by the dotted lines, and the average is the solid black line.

As the threshold parameter, α_0 , increases, so does the coefficient of variation. The coefficient of variation represents the ratio of the standard deviation to the mean of the data giving a value to represent the variability in the data set. As α_0 increases, the dispersion in data also increases. This means the more data is removed (randomly), the higher the variability in the results. This is depicted even more so in the graph below:

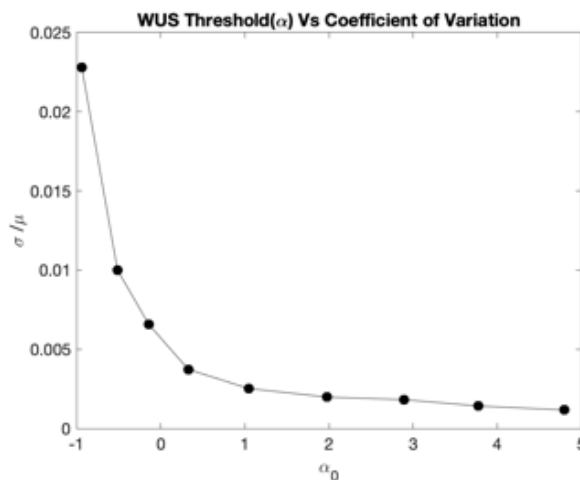


Figure 20 - This is the coefficient of variation (σ/μ) versus α_0 of the estimated PGA at 2% exceedance probability in 50 years. Depicting that as α_0 increases there is less variation in the data.

With an increase in the number of events kept, there is a decrease in the variability of the data due to the smaller impact of the random thinning process.

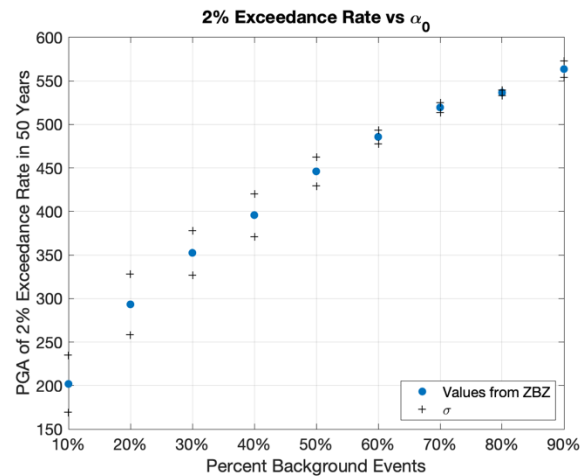


Figure 21- This graph shows the average exceedance rates for all of the 100 runs per percentage of catalog kept along with the standard deviation values. As the number of events in the catalog increases, the variability in the data decreases.

As α_0 shifts, the hazard estimate for the location changes. With more significant percentages of the catalog defined as independent, the higher the hazard rating for the areas. A higher hazard rating is the increase in risk and level of earthquake activity in a particular region or area. The hazard plots below show three separate curves: the USGS hazard curve, the simplified approximation, and the Zaliapin & Ben-Zion declustered catalog curve. As the number of events in the catalog increased, so did the hazard curve values.

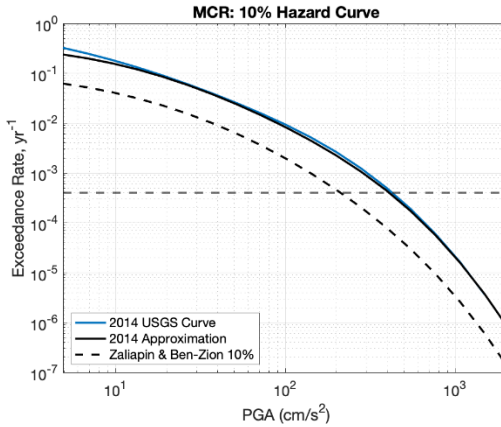


Figure 22 - This depicts hazard curves of 10% of the seismic catalog removed. The John Anderson smoothing algorithm simplifies the complicated logic tree the USGS uses to predict hazard. This plot comparison relays the simplification is reasonable.

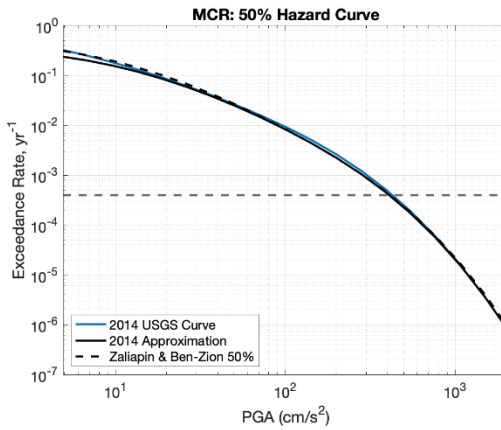


Figure 23 - This depicts hazard curves of 50% of the seismic catalog removed. The John Anderson smoothing algorithm simplifies the complicated logic tree the USGS uses to predict hazard. This plot comparison relays the simplification is reasonable.

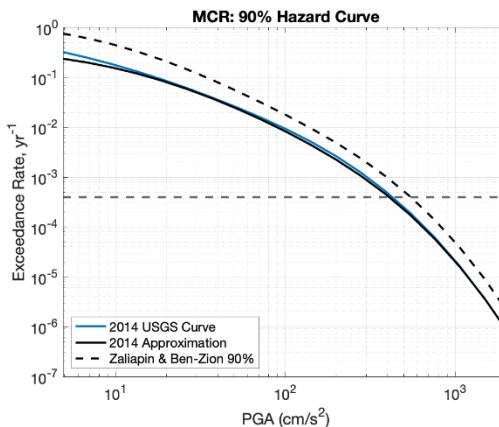


Figure 24 - This depicts hazard curves of 90% of the seismic catalog removed. The John Anderson smoothing algorithm simplifies the complicated logic tree the USGS uses to predict hazard. This plot comparison relays the simplification is reasonable.

Discussion

Seismic hazard is assessed to provide the best estimate for seismic events to occur in a specific area. Hazard analysis should be as accurate as possible to avoid excess costs incurred during building or from future earthquake damage. Declustering has been a crucial step in seismic hazard analysis, as engineers, city planners, and others design for engineered structures to withstand the most likely amount of ground shaking.

The Zaliapin and Ben-Zion (ZBZ) method allowed multiple iterations of declustering on a seismic catalog, randomly thinning it; this allows the background seismicity to maintain its randomness. By plotting multiple iterations of the same catalog with different α_0 values, we were able to show how the hazard varies through different events in the catalog.

Contour Maps

Contouring the declustered catalogs against the original catalog show where events are removed. It also allows for comparison against the USGS's declustered catalog, c3. The USGS declustered catalog has roughly 38% of the original catalog. I created a catalog with 38% background events using the ZBZ declustering algorithm for a more direct comparison. Figure 13 and 14 are a depiction of this.

Comparing the c3 catalog to the 38% ZBZ declustered catalog shows the differences in event removal. Looking along the Nevada-California border, the c3 catalog has a larger area with more events removed. The ZBZ catalog has more events removed in areas with higher earthquake density.

The contour maps suggest that ZBZ removes events in already seismically dense areas compared to the USGS declustered c3 catalog, which has a more "dispersed" looking declustering. Since ZBZ uses a nearest-neighbor method I conclude this contributes to having more events removed in areas where there are more events and leaving events that are farther out to be considered independent.

That being said, I would like to know whether, in a different region with varying types of seismicity, should different types of declustering be used. The next step would be to determine where different methods remove different proportions of events.

Hazard Curves (Iterations)

Throughout 100 different catalog versions, the solutions tend to merge to the same result for the hazard curves. Generally, the hazard curves are stable with respect to the random thinning. With more events in the catalog, the variability in the curve itself is lower. With an α_0 that is "pickier," different events are defined as independent; this variability comes from which events are selected for the catalog. This random thinning allows for holes to be filled in after a more significant event, because the catalog is being thinned due to a threshold parameter rather than a time-space window like other methods.

The probability of exceeding a certain PGA is higher when keeping more events in the seismic catalog. With more events in the catalog, variability in the PGA decreases.

Hazard Curves Comparisons

This study demonstrates that an increase in the number of events in a seismic catalog corresponds to a higher hazard estimate for the area while removing more events results in a lower hazard. An interesting insight emerged from comparing hazard curves across the United States West Coast. However, the accuracy of these curves may need to be revised. In locations like Santa Cruz and Mammoth Lakes, California, the ZBZ catalog yielded hazard curves similar to the 2018 USGS results. However, the ZBZ method produced considerably lower hazard estimates for areas near significant fault lines such as in Salt Lake City, Utah. This disparity could be attributed to variations in the catalog smoothing methodology used in this study compared to the PSHA report's methodology.

Conclusion

In conclusion, this project has delved into the relationship between declustering techniques and earthquake hazard estimations, focusing on the potential impact on the USGS National Seismic Hazard Model (NSHM). I have found insights by implementing a novel declustering technique developed by Zaliapin & Ben-Zion (2020), which allows for manipulating background events while preserving spatial inhomogeneous distribution.

One significant revelation is that the hazard estimations remain consistent across various stochastic realizations of declustering for the same average number of background events. This finding underscores the methodology's robustness and the hazard assessments' reliability.

Furthermore, my research has illuminated the direct correlation between the number of background events retained in the catalog and the resulting earthquake hazard. In the case of the Monte Cristo Range Earthquake, maintaining approximately 38% of the background events aligns

the hazard curves with those generated by the USGS. This highlights the practical implications of declustering techniques in shaping hazard estimations.

Altering the proportion of background events within the catalog from 10% to 90% led to a substantial variation in the estimated peak ground acceleration (PGA) at a 2% exceedance probability over 50 years. The variations ranged from 200 cm/s² to 550 cm/s², with the USGS value at 420 cm/s². This finding emphasizes the critical role of declustering in accurately characterizing earthquake hazards, especially when the proportion of background events varies significantly.

Ultimately, the research has highlighted a fundamental relationship: the more events retained in the catalog, the higher the hazard for a given area. This insight underscores the significance of declustering methods in seismic hazard assessment and emphasizes that the overall hazard output remains consistent regardless of stochastic variations.

In sum, this project not only advances our understanding of the relationship between declustering techniques and earthquake hazard estimations but also offers practical implications for enhancing the accuracy and reliability of seismic hazard assessments. The findings presented here contribute to the broader body of knowledge in seismology and have the potential to inform and improve earthquake preparedness and mitigation strategies.

Summary

This paper discusses declustering and how it affects hazard estimations. A multiple-step process determines the seismic hazard for a given area. The USGS updates a hazard map for the United States every seven years. With advances in technology and the collection of more data, the methods for creating this hazard assessment update with every iteration.

Declustering is a controversial step in the analysis of seismic hazard. This initial step in seismic hazard analysis removes events classified as dependent, meaning the events proceed or follow a larger event. Different methods of declustering classify events as dependent or independent with

varying algorithms and parameters. The method of declustering used in this study allows the user to vary the number of background events while preserving the estimated spatial inhomogeneous distribution of the background. *Zaliapin & Ben-Zion* published this method in 2020. This method was optimal for this study as the number of events kept in the catalog could be varied quickly and easily.

Suggested Follow Up Work

The next step to further this analysis is completing the same steps with a more extensive data set. A more complete data set would provide more insight into where the events are removed. With the older catalog not being as complete, the ZBZ declustering would be inaccurate due to the nearest neighbor calculations. There is insufficient information to decide whether declustering is necessary. Not only necessary but also if this is the correct method (ZBZ) for declustering.

It would be helpful to do this for the eastern United States as well to see how it compares in an area that is not Nevada. This would help determine how the algorithm works in areas that have not just background seismicity as the main seismic contribution.

It is interesting to look at the contour maps and see that different amounts of events are removed with different declustering methods. Running multiple different declustering methods to compare contour maps to see where events are removed from would be an informative next step. This could lead to a fascinating insight into where and how to use declustering.

Data Used

- Catalogs retrieved from USGS:
 - <https://www.sciencebase.gov/catalog/item/5b1813c1e4b092d965219a1c>
 - <https://www.sciencebase.gov/catalog/item/5d559635e4b01d82ce8e3fe7>

References

- Anderson, John, and Ilia Zaliapin. "Final Technical Report USGS Award Number G20AP00010 Effects of Earthquake Declustering on the US National Seismic Hazard Maps.
- Baiesi, Marco & Paczuski, Maya. (2004). Scale-free networks of earthquakes and aftershocks. *Phys. Physical review. E, Statistical, nonlinear, and soft matter physics.* 69. 066106. 10.1103/PhysRevE.69.066106.
- Budnitz, R. J., G. Apostolakis, and David M. Boore. Recommendations for probabilistic seismic hazard analysis: guidance on uncertainty and use of experts. No. NUREG/CR-6372-Vol. 1; UCRL-ID-122160. US Nuclear Regulatory Commission (NRC), Washington, DC (United States). Div. of Engineering Technology; Lawrence Livermore National Lab.(LLNL), Livermore, CA (United States); Electric Power Research Inst.(EPRI), Palo Alto, CA (United States); US Department of Energy (USDOE), Washington DC (United States), 1997.
- Cornell, C. Allin. "Engineering seismic risk analysis." *Bulletin of the seismological society of America* 58.5 (1968): 1583-1606.
- Christophersen, A., et al. "Quantifying the effect of declustering on probabilistic seismic hazard." *Proc. of the Ninth Pacific Conf. on Earthquake Engineering: Building an Earthquake-Resilient Society.* 2011.
- "Earthquake Hazards 101 - the Basics | U.S. Geological Survey", United States Geologic Survey 6 Aug. 2019, www.usgs.gov/programs/earthquake-hazards/science/earthquake-hazards-101-basics.
- "Earthquake Hazards Overview." *Pacific Northwest Seismic Network*, Pacific Northwest Seismic Network, pnsn.org/outreach/earthquakehazards. Accessed 4 Dec. 2023.
- Gardner, J. K., & Knopoff, L. (1974). Is the sequence of earthquakes in Southern California, with aftershocks removed, Poissonian? *Bulletin of the Seismological Society of America*,

64(5), 1363–1367.

Marsan, D., and O. Lengline, 2008, Extending Earthquakes' Reach Through Cascading, *Science*, 319(5866), 1076-1079, doi:10.1126/science.1148783.

Marsan, D., and O. Lengline, 2010, A new estimation of the decay of aftershock density with distance to the mainshock, *Journal of Geophysical Research*, *in press*.

Mueller, C.S., 2018, Earthquake Catalogs for the USGS National Seismic Hazard Maps: *Seismological Research Letters*, 90(1), 251-261.

Petersen MD, Shumway AM, Powers PM, et al. The 2018 update of the US National Seismic Hazard Model: Overview of model and implications. *Earthquake Spectra*. 2020;36(1):541. doi:[10.1177/8755293019878199](https://doi.org/10.1177/8755293019878199)

Reasenber, P., 1985, Second-order moment of central California seismicity, 1969-82, *J. Geophys. Res.*, 90, 5479-5495.

Reiter, L. (1990). *Earthquake Hazard. Analysis: Issues and Insights* (p. 254). Columbia University Press.

Rukstales, K.S., and Petersen, M.D., 2019, Data Release for 2018 Update of the U.S. National Seismic Hazard Model: U.S. Geological Survey data release, <https://doi.org/10.5066/P9WT5OVB>.

van Stiphout, T., J. Zhuang, and D. Marsan (2012), Seismicity declustering, Community Online Resource for Statistical Seismicity Analysis, doi:[10.5078/corssa-52382934](https://doi.org/10.5078/corssa-52382934). Available at <http://www.corssa.org>

Zaliapin, I., & Ben-Zion, Y. (2020). Earthquake declustering using the nearest-neighbor approach in space time-magnitude domain. *Journal of Geophysical Research: Solid Earth*, 125, e2018JB017120. <https://doi.org/10.1029/2018JB017120>

Zhuang, J., Y. Ogata, and D. Vere-Jones (2002), Stochastic declustering of space-time earthquake occurrences, *J. Am. Stat. Assoc.*, 97, 369-380. http://www.corssa.org/glossary/#Omori-Utsu_relation

Appendix

Epicenter of Events with Time verse Latitude

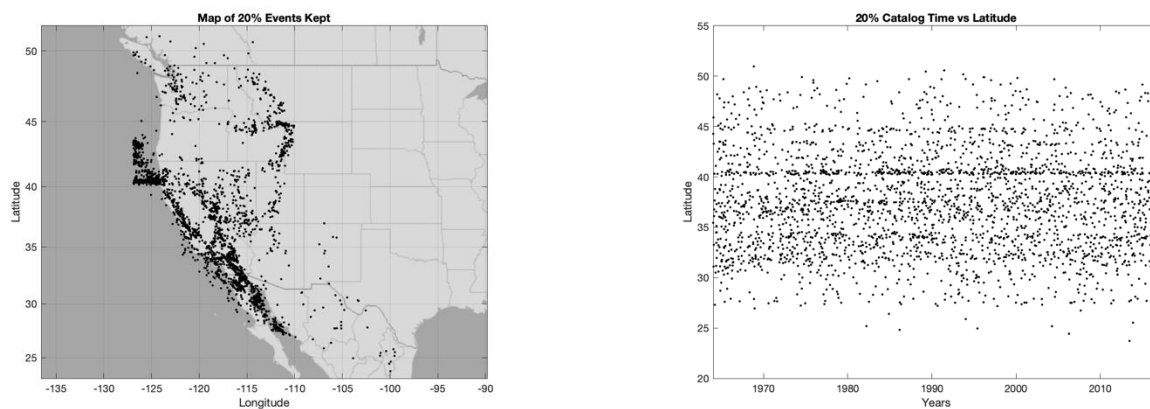


Figure A-1: Epicenters of the ZBZ catalog with 20% of background events kept. Adjacent to a scatter plot of the same catalog epicenters plotted against latitude versus years.

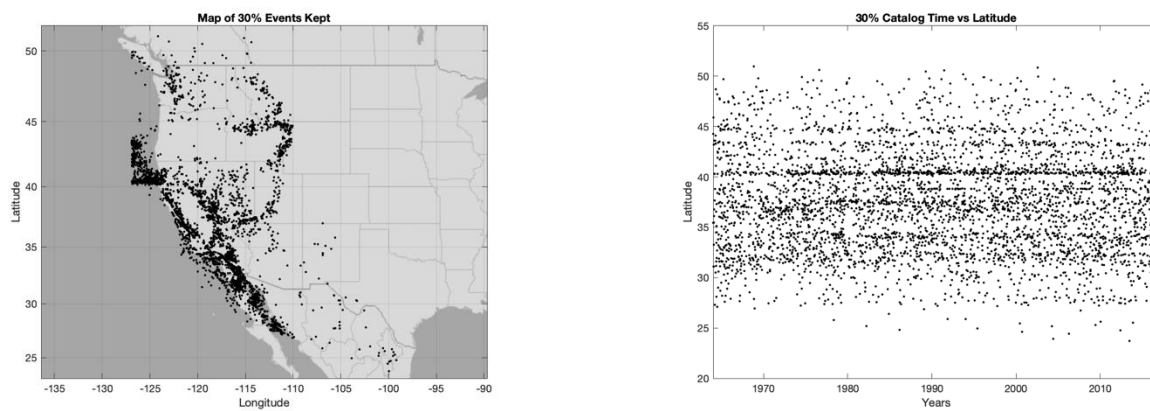


Figure A-2: Epicenters of the ZBZ catalog with 30% of background events kept. Adjacent to a scatter plot of the same catalog epicenters plotted against latitude versus years.

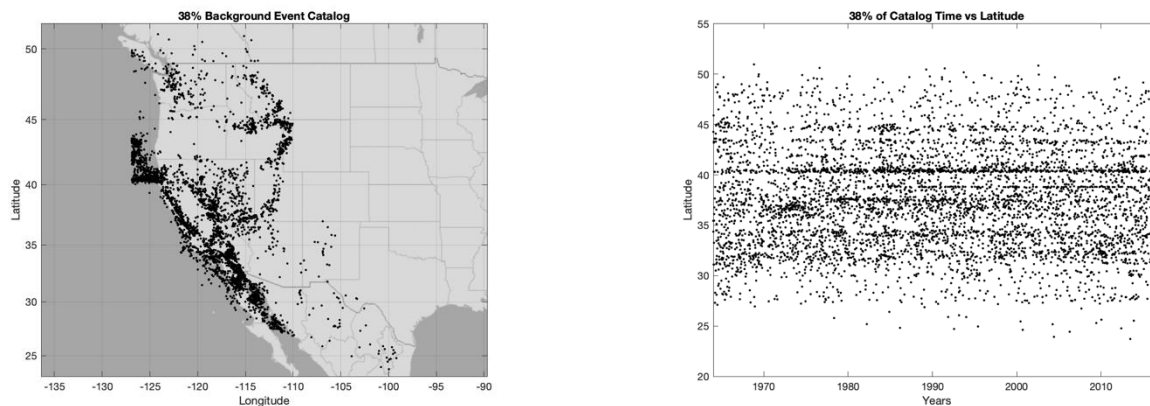


Figure A-3: Epicenters of the ZBZ catalog with 38% of background events kept. Adjacent to a scatter plot of the same catalog epicenters plotted against latitude versus years.

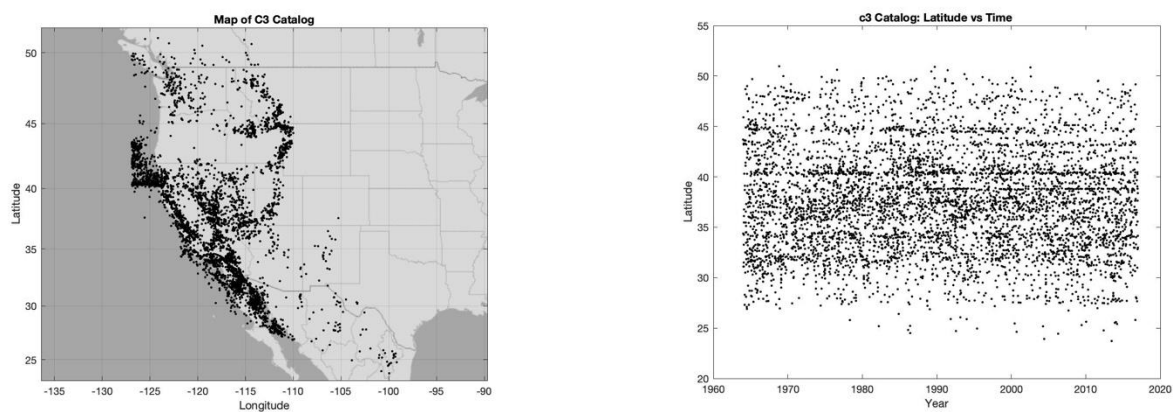


Figure A-4: Epicenters of the c3 catalog with the background events kept. Adjacent to a scatter plot of the same catalog epicenters plotted against latitude versus years.

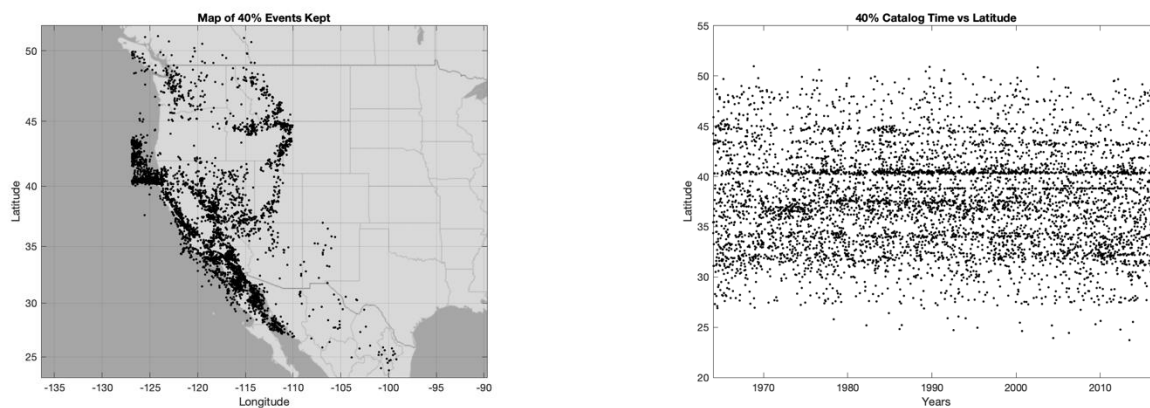


Figure A-5: Epicenters of the ZBZ catalog with 40% of background events kept. Adjacent to a scatter plot of the same catalog epicenters plotted against latitude versus years.

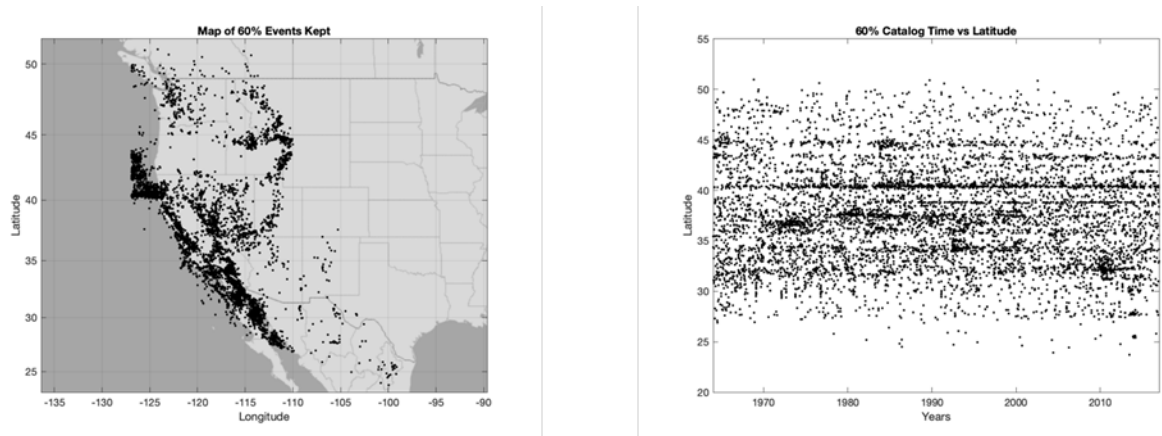


Figure A-6: Epicenters of the ZBZ catalog with 60% of background events kept. Adjacent to a scatter plot of the same catalog epicenters plotted against latitude versus years.

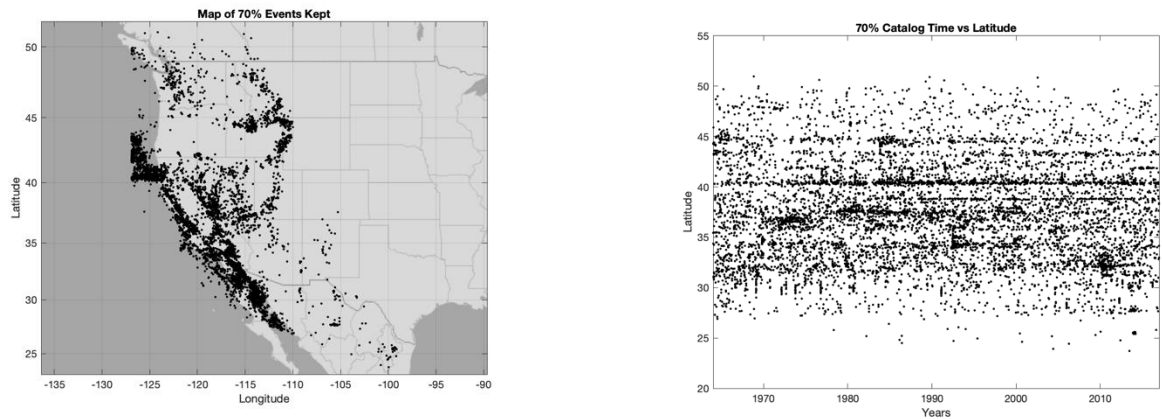


Figure A-7: Epicenters of the ZBZ catalog with 70% of background events kept. Adjacent to a scatter plot of the same catalog epicenters plotted against latitude versus years.

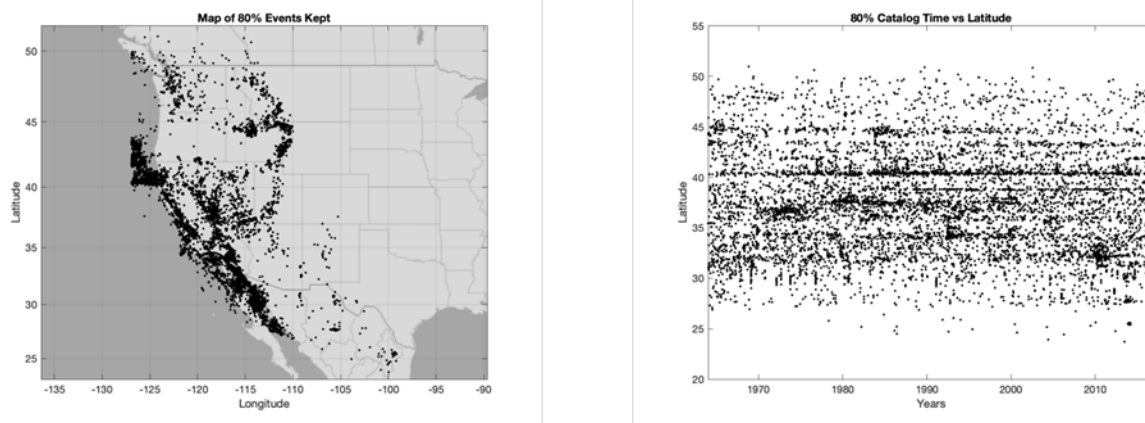


Figure A-8: Epicenters of the ZBZ catalog with 80% of background events kept. Adjacent to a scatter plot of the same catalog epicenters plotted against latitude versus years.

Contour Maps showing where events are removed from catalog.

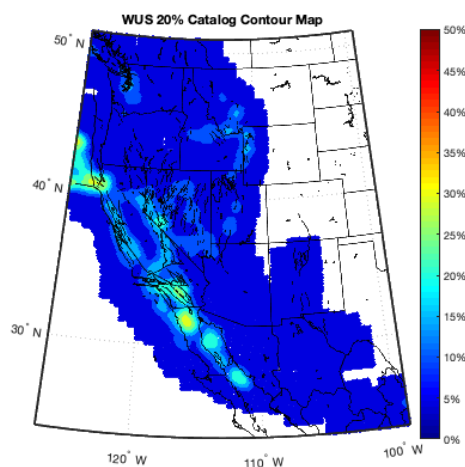


Figure A-9: Contour map of ZBZ declustered catalog removing 20% of background events from the c2 catalog. To compare the same amount of events removed by the USGS declustering versus the ZBZ declustering. This depicts where the ZBZ declustering method removes earthquakes.

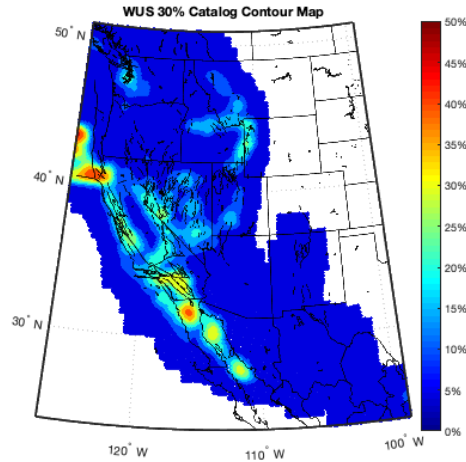


Figure A-10: Contour map of ZBZ declustered catalog removing 30% of background events from the c2 catalog. To compare the same amount of events removed by the USGS declustering versus the ZBZ declustering. This depicts where the ZBZ declustering method removes earthquakes.

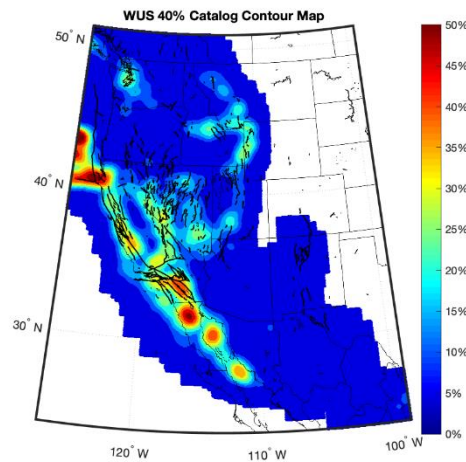


Figure A-11: Contour map of ZBZ declustered catalog removing 40% of background events from the c2 catalog. To compare the same amount of events removed by the USGS declustering versus the ZBZ declustering. This depicts where the ZBZ declustering method removes earthquakes.

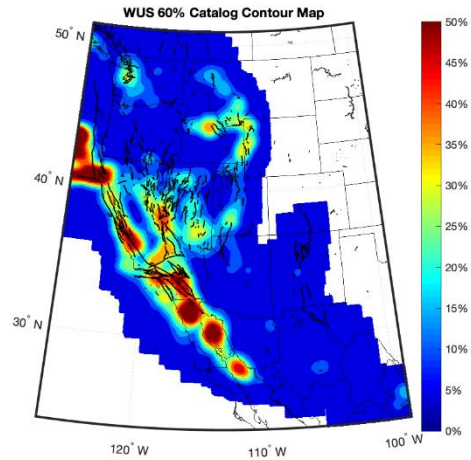


Figure A-12: Contour map of ZBZ declustered catalog removing 60% of background events from the c2 catalog. To compare the same amount of events removed by the USGS declustering versus the ZBZ declustering. This depicts where the ZBZ declustering method removes earthquakes.

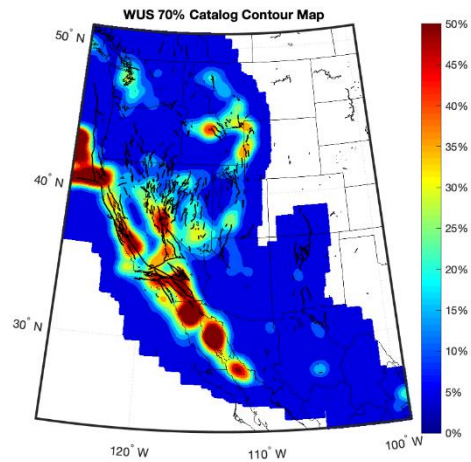


Figure A-13: Contour map of ZBZ declustered catalog removing 70% of background events from the c2 catalog. To compare the same amount of events removed by the USGS declustering versus the ZBZ declustering. This depicts where the ZBZ declustering method removes earthquakes.

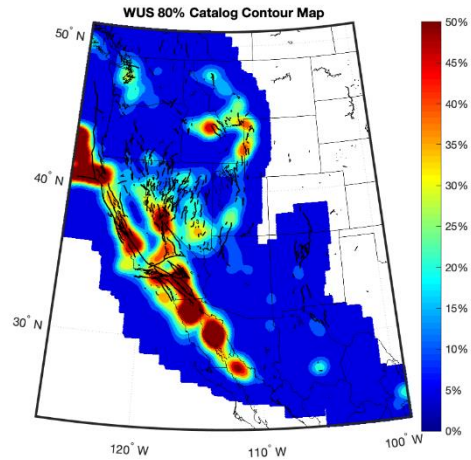


Figure A-14: Contour map of ZBZ declustered catalog removing 80% of background events from the c2 catalog. To compare the same amount of events removed by the USGS declustering versus the ZBZ declustering. This depicts where the ZBZ declustering method removes earthquakes.

Hazard Curves with Multiple Catalog Realizations

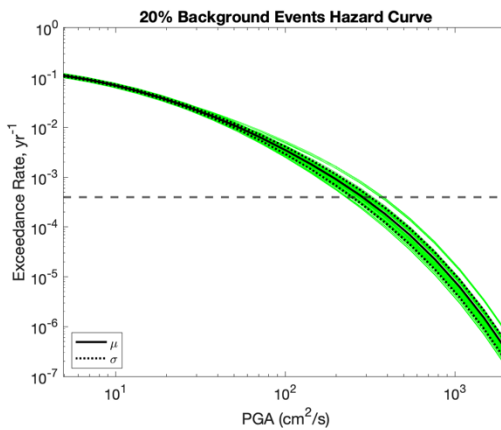


Figure A-15: Hazard Curve of 20% of events removed from seismic catalog. The green lines represent 100 different realizations of 20% of events being removed. Standard deviation is shown by the dotted lines, and the average is the solid black line.

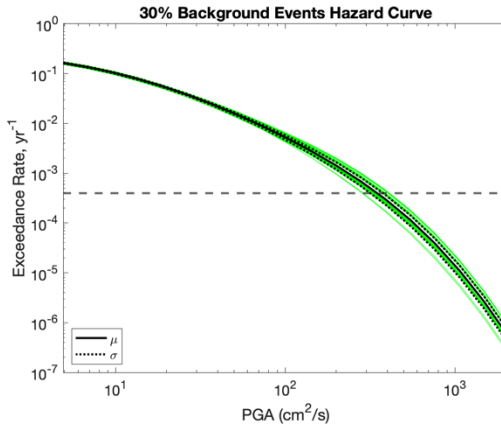


Figure A-16: Hazard Curve of 30% of events removed from seismic catalog. The green lines represent 100 different realizations of 30% of events being removed. Standard deviation is shown by the dotted lines, and the average is the solid black line.

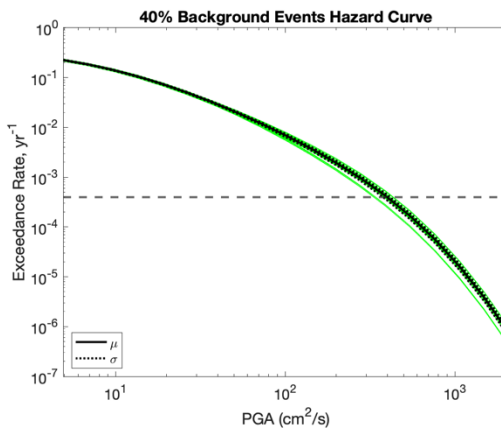


Figure A-17: Hazard Curve of 40% of events removed from seismic catalog. The green lines represent 100 different realizations of 40% of events being removed. Standard deviation is shown by the dotted lines, and the average is the solid black line.

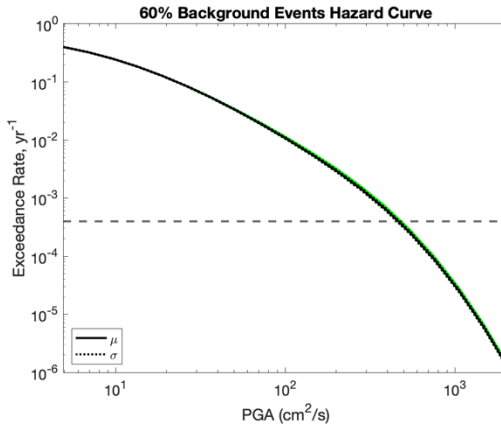


Figure A-18: Hazard Curve of 60% of events removed from seismic catalog. The green lines represent 100 different realizations of 60% of events being removed. Standard deviation is shown by the dotted lines, and the average is the solid black line.

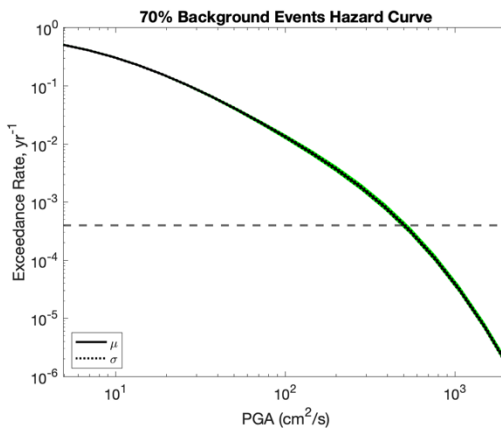


Figure A-19: Hazard Curve of 70% of events removed from seismic catalog. The green lines represent 100 different realizations of 70% of events being removed. Standard deviation is shown by the dotted lines, and the average is the solid black line.

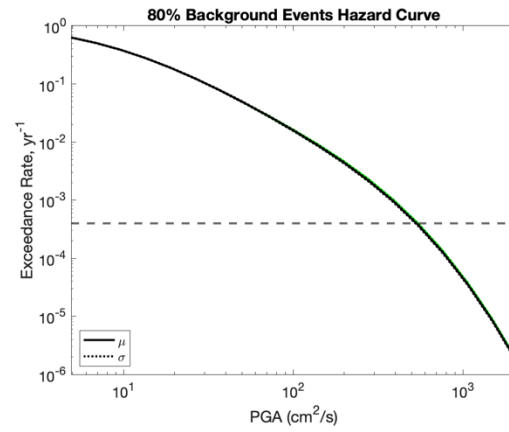


Figure A-20: Hazard Curve of 80% of events removed from seismic catalog. The green lines represent 100 different realizations of 80% of events being removed. Standard deviation is shown by the dotted lines, and the average is the solid black line.

Hazard Curve of ZBZ Method compared to Actual Curves and Estimate

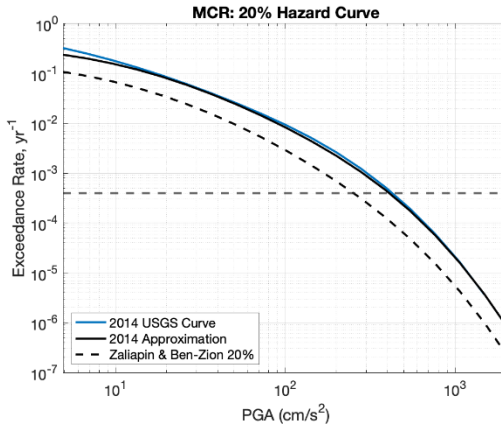


Figure A-21: This depicts hazard curves of 20% of the seismic catalog removed. The John Anderson smoothing algorithm simplifies the complicated logic tree the USGS uses to predict hazard. This plot comparison relays the simplification is reasonable.

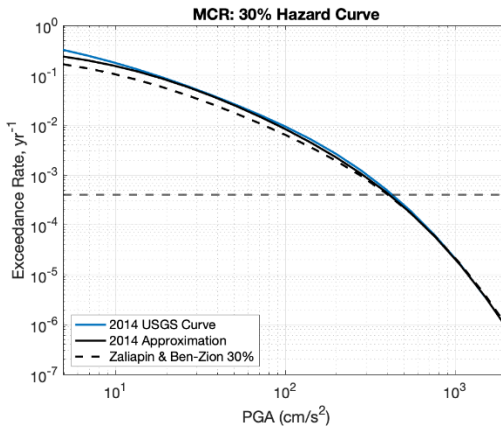


Figure A-22: This depicts hazard curves of 30% of the seismic catalog removed. The John Anderson smoothing algorithm simplifies the complicated logic tree the USGS uses to predict hazard. This plot comparison relays the simplification is reasonable.

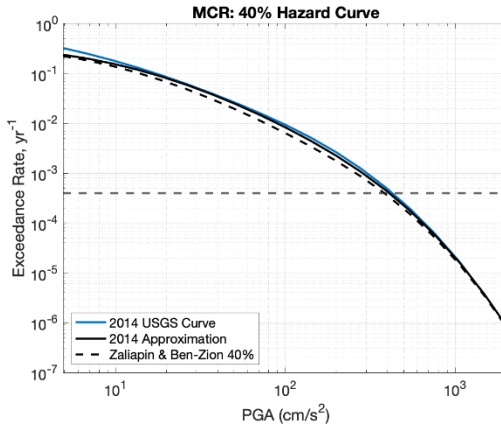


Figure A-23: This depicts hazard curves of 40% of the seismic catalog removed. The John Anderson smoothing algorithm simplifies the complicated logic tree the USGS uses to predict hazard. This plot comparison relays the simplification is reasonable.

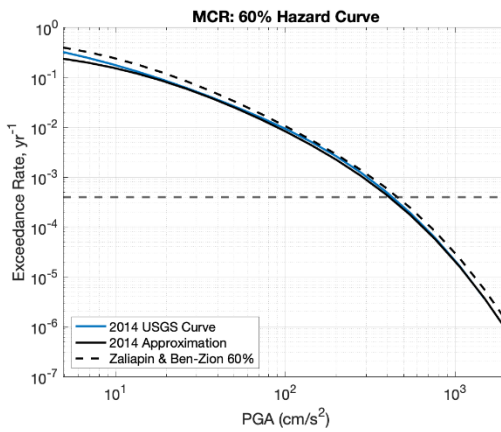


Figure A-24: This depicts hazard curves of 60% of the seismic catalog removed. The John Anderson smoothing algorithm simplifies the complicated logic tree the USGS uses to predict hazard. This plot comparison relays the simplification is reasonable.

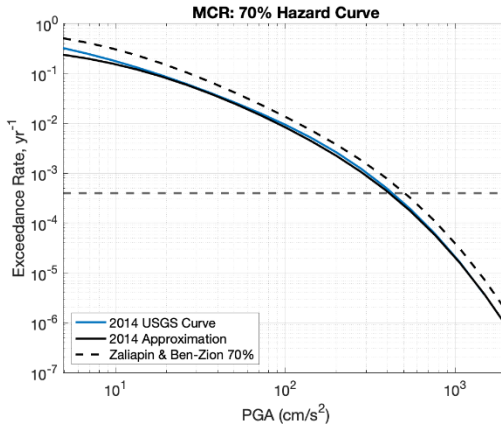


Figure A-25: This depicts hazard curves of 70% of the seismic catalog removed. The John Anderson smoothing algorithm simplifies the complicated logic tree the USGS uses to predict hazard. This plot comparison relays the simplification is reasonable.

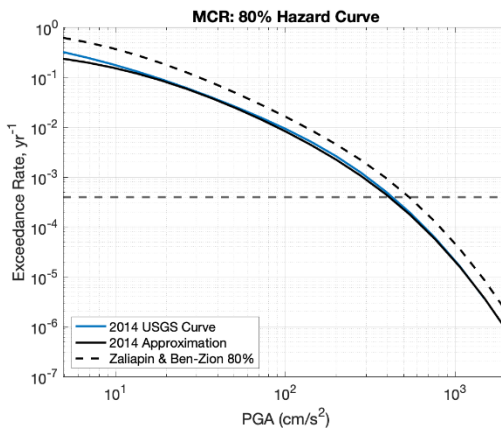


Figure A-26: This depicts hazard curves of 80% of the seismic catalog removed. The John Anderson smoothing algorithm simplifies the complicated logic tree the USGS uses to predict hazard. This plot comparison relays the simplification is reasonable.